J Therm Anal Calorim (2012) 110:545–550
DOI 10.1007/s10973-012-2541-x

Solid–liquid equilibria, thermochemical and microstructural studies of binary organic monotectic and eutectic alloy

K. P. Sharma · R. S. B. Reddi · R. N. Rai

SATAC-ACT2011 Conference Special Chapter

Abstract The phase diagram of 1,4-dibromobenzene (DBB) with pyrogallol (PG) shows the formation of a monotectic and a eutectic alloys at 0.12 and 0.99 mol fractions of DBB, respectively. The phase equilibrium shows the large miscibility gap region with the upper consolute temperature 159.0 °C at 0.55 mol fraction of DBB. Growth kinetics of pure compounds and their monotectic and eutectic at different undercooling (ΔT) obey Hillig–Turnbull's equation: $v = u\ (\Delta T)^n$. Thermodynamic parameters such as enthalpy of mixing, entropy of fusion, interfacial energy, roughness parameters and excess thermodynamic functions were computed based on enthalpy of fusion values obtained from DSC studies. The Cahn wetting condition is applicable for monotectic alloy. The optical microphotographs of binary alloys show lamellar and dendritic features.

Keywords Phase equilibria · Thermochemistry · Microstructure · Heat of fusion · Monotectics · Interfacial energy

Introduction

To cater the needs of current civilization, science demands newer materials with special features at low cost. The metallic systems and their alloys were found to be potential candidates for technological applications. However, the limited choice of materials, difficulties in experimentation, high density difference, opacity in vision during phase transformation and high transformation temperature and cost were the limiting factors to work with the metallic systems [1–3]. The organic eutectics, monotectics and addition compounds, which could be considered as organic analogs of metallic eutectics, monotectics and intermetallic compounds [4–6], have gained potential importance due to low transformation temperature, ease of purification, transparency, minimized convection effects and wider choice of materials. The number of research groups [7–10] is actively investigated on organic systems as the model systems. Now-a-days, these systems are known for their promising NLO, fluorescence, and conducting behavior which reinforce the investigation to produce the specific materials for their device applications. The solidification behavior of monotectic alloy is of potential importance for fundamental understanding as well as for development of self-lubricating alloys and industrial applications. The role of wetting behavior, interfacial energy, thermal conductivity and buoyancy in a phase separation process of monotectic has been a subject of great discussion. However, the monotectic alloys have been studied very less due to several difficulties associated with the miscibility gap systems. In this communication, the phase diagram, solidification behavior, thermochemistry, and microstructures of 1,4-dibromobenzene-pyrogallol system are being communicated.

K. P. Sharma · R. S. B. Reddi · R. N. Rai (✉)
Department of Chemistry, Centre of Advanced Study, Banaras Hindu University, Varanasi 221 005, India
e-mail: rn_rai@yahoo.co.in

K. P. Sharma
Department of Chemistry, Butwal Multiple Campus, Tribhuvan University, Butwal, Nepal

Experimental

Materials and purification

1,4-Dibromobenzene (Fluka, Switzerland) was purified by crystallization from diethyl ether, while pyrogallol

(Thomas Baker, India) was purified by recrystallization from ethanol. The purity of each compound was checked by determining their melting points and comparing with the literature values. The experimental values of melting points of DBB and PG were found to be 87.5 and 133.0 °C, respectively, which are fairly close to their reported values 87.4 and 133.0 °C, respectively.

Phase diagram

The phase diagram of DBB–PG system was established in the form of temperature–composition curve [5]. The mixtures of two components covering the entire range of compositions were prepared and these mixtures were homogenized by repeating the process of melting followed by chilling in ice-cold water for 3–4 times. The melting points of completely miscible compositions and the miscibility temperatures of mixtures showing miscibility gap were determined using a melting point measuring apparatus attached with a precision thermometer of accuracy ±0.5 °C.

Enthalpy of fusion

The values of heat of fusion of the pure components, the eutectic and the monotectic were determined [5] by differential scanning calorimeter (Mettler DSC-4000 system). Indium sample was used to calibrate the system and the amount of test sample and heating rate were about 6.0 mg and 10 °C min^{-1}, respectively, for each estimation. The values of enthalpy of fusion are reproducible within ±1.0 %.

Growth kinetics

For the study of growth kinetic, the linear velocity of crystallization of the pure components, the eutectic and the monotectic was determined [11, 12] at different particular temperatures. The rate of movement of the solid–liquid interface was determined in a thin glass *U*-tube (150 mm horizontal portion and 4 mm internal diameter) fitted with a scale. The entire setup was kept in a silicone oil bath, and the temperature of oil bath was maintained using microprocessor temperature controller which could control and read up to ±0.1 °C. At each undercooling, to facilitate the nucleation, a seed crystal of the same material was added at the one end of the *U*-tube and the rate of movement of the crystallizing front was recorded using a stopwatch and a sliding microscope.

Microstructure

Microstructures of the pure components, the eutectic, and the monotectic were recorded by placing a drop of molten sample on a hot glass slide [12]. A cover slip was glided over the melt and it was allowed to solidify unidirectionally. The slide was placed on the platform of an optical microscope (Leitz Labourlux D), different regions were viewed and interesting regions were photographed with suitable magnification of camera attached with the microscope.

Results and discussions

Phase diagram

The phase diagram of DBB–PG system, established between compositions and their melting/miscibility temperatures has been depicted in Fig. 1 which shows the formation of a monotectic and a eutectic. Melting point of PG is 133.0 °C and it decreases on the addition of DBB. When the mole fraction of DBB reaches 0.12, the melts of DBB and PG appears immiscible and at a certain temperature, these two liquids become completely miscible. With an increase in composition of DBB, the miscibility temperature also increases and attains a maximum value when the mole fraction of DBB reaches 0.55. The maximum miscibility temperature (159.0 °C) is also known as the

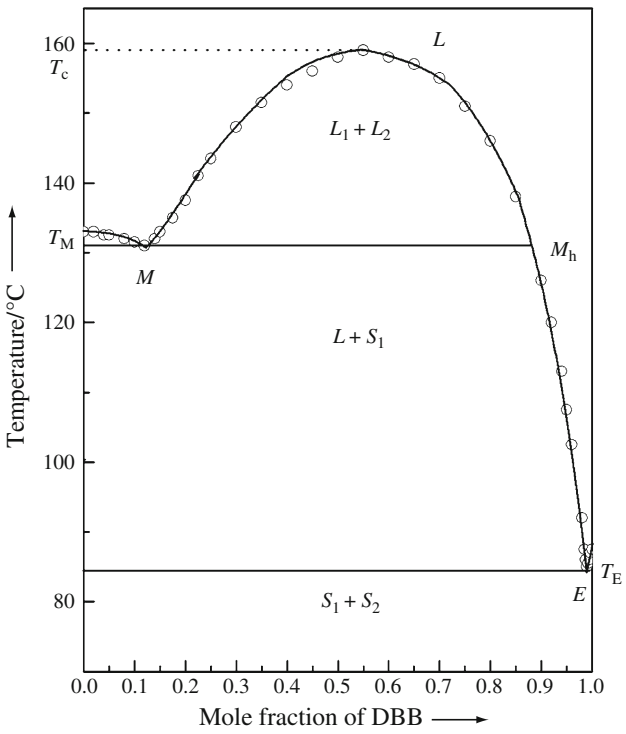

Fig. 1 Phase diagram of 1,4-dibromobenzene–pyrogallol system o Melting/miscibility temperature, *L*-Liquid phase, L_1-Liquid phase of pyrogallol, S_1-Solid phase of pyrogallol, L_2-Liquid phase of 1,4-dibromobenzene, and S_2-Solid phase of 1,4-dibromobenzene

upper consolute/critical temperature (T_c), which is 28.0 °C above the monotectic horizontal (M_h). Both the components are miscible in all proportions above this critical temperature. The thermal study of different compositions reveals that there are three reactions of interest, which occur isothermally on solidification. The first reaction concerns the phase separation in two liquids when the liquid of single phase, above 159.0 °C, is cooled below the critical temperature (T_c), as

$$L \leftrightarrow L_1 + L_2$$

The second reaction, known as monotectic reaction, is quite similar to the eutectic reaction except that one of the product phases is a second liquid L_2, as follows:

$$L_1 \leftrightarrow S_1 + L_2$$

The third reaction is the eutectic reaction in which the liquid L_2 decomposes to give two solids as

$$L_2 \leftrightarrow S_1 + S_2$$

The monotectic, the eutectic and the critical solution temperatures in the present case are 131.0, 85.0, and 159.0 °C, respectively. The monotectic and the eutectic point are the invariant points.

Growth kinetics

In order to study the crystallization behavior of the pure components, the eutectic and the monotectic, the crystallization rate (v) have been determined at different undercoolings (ΔT) by measuring the rate of movement of solid–liquid interface in a capillary. The plots between log ΔT and log v, for different materials, are given in Fig. 2 and the linear dependence of these plots are in accordance with Hillig–Turnbull equation [13]

$$v = u(\Delta T)^n \quad (1)$$

where u and n are constants and depend on the solidification behavior of the materials involved. The experimental values of these constants are given in Table 1.

The u value is a measure of the linear velocity of crystallization of the concerned material. It is evident from the values of u that the linear velocity of crystallization of the eutectic and monotectic both lie in between those of the pure components, representing a similar trend in the growth velocity. These variations are explained by the mechanism proposed by Winegard et al. [14]. According to them, the eutectic solidification begins with the formation of nucleus of one of the phases. This would grow until the surrounding liquid becomes rich in the other component and a stage is reached when the second component also starts nucleating. Thus, there are two possibilities: either the two initial crystals may grow side by side or there may be alternate

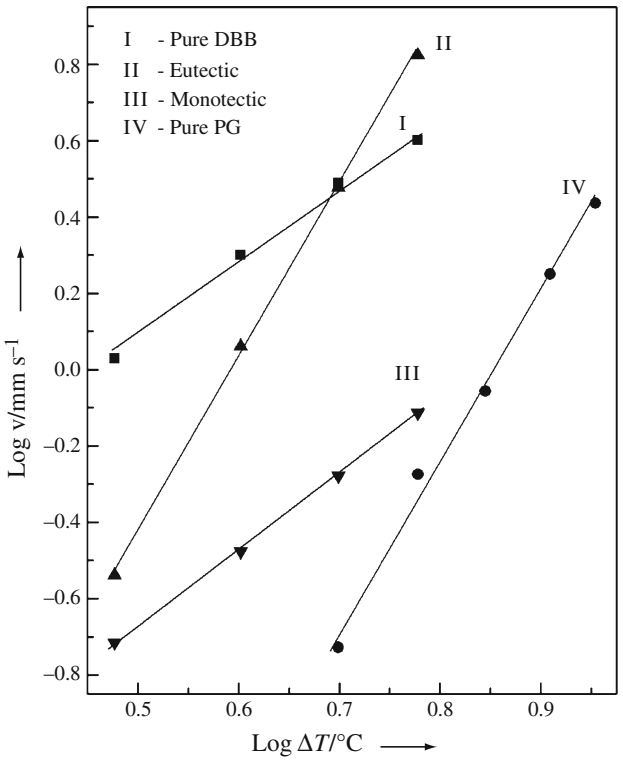

Fig. 2 Linear velocity of crystallization at various undercooling for 1,4-dibromobenzene, pyrogallol, and their monotectic and eutectic

nucleation of the two components. The side by side nucleation mechanism explains the intermediate growth velocity of the binary materials in comparison to the pure components. It is observed in the DBB–PG system that the u value for the monotectic is smaller than the eutectic. Both eutectic and monotectic follow the side by side nucleation mechanism as their u values are in between the parent components. The difference between the growth velocity of eutectic and monotectic may be due to the difference of mode of heat flow and diffusion during the solidification of monotectic and eutectic.

Thermochemistry

Enthalpy of fusion

The values of enthalpy of fusion of the pure components, the eutectic and the monotectic are determined by the DSC method and have been reported in Table 1. For comparison, the value of enthalpy of fusion of eutectic calculated by the mixture law [15] is also included in the same table. The enthalpy of mixing, which is the difference of experimental and calculated values of the enthalpy of fusion, is found to be 1.76 kJ mol^{-1}. The positive value of ΔH_{mix} for the eutectic of the present system suggests the quasi-

Table 1 Heat of fusion, entropy of fusion, roughness parameter, and values of u and n for pure components, monotectic, and eutectic

Materials	Heat of fusion/kJ mol^{-1}	Entropy of fusion/J mol^{-1} K^{-1}	Roughness parameter/α	u/mm s^{-1} deg^{-1}	n
DBB	20.60	57.14	6.87	1.35×10^{-1}	1.92
PG	23.90	59.09	7.11	1.54×10^{-4}	4.46
Monotectic	25.31	62.65	7.54	2.12×10^{-2}	2.00
Eutectic (Exp.)	22.39	62.54	6.52	2.11×10^{-3}	4.51
(Cal.)	20.63				

eutectic structure in the binary eutectic melt [5]. The entropy of fusion (ΔS_{fus}) values, for different materials have been calculated by dividing the enthalpy of fusion by their corresponding absolute melting temperatures (Table 1). The values of the entropy of fusion being positive suggest that there is an increasing randomness of the system during melting as expected. The higher value of entropy of fusion of eutectic suggests an increasing randomness in eutectic melt.

Size of critical nucleus and interfacial energy

When liquid is cooled below its melting temperature, it does not solidify spontaneously, because under equilibrium condition the melt contains number of clusters of molecules of different sizes. As long as the clusters are well below the critical size, they cannot grow to form crystals, and no solid would result. The critical size (r^*) of nucleus [15] is related to interfacial energy (σ) by the equation,

$$r^* = \frac{2\sigma T_{\text{fus}}}{\Delta H_{\text{fus}} \Delta T} \tag{2}$$

where T_{fus}, ΔH_{fus}, and ΔT are melting temperature, heat of fusion, and degree of undercooling, respectively. An estimate of the interfacial energy [11] is given by the expression

$$\sigma = \frac{C \Delta H_{\text{fus}}}{(N_{\text{A}})^{1/3} (V_{\text{m}})^{2/3}} \tag{3}$$

where N_{A} is the Avogadro number, V_{m} is the molar volume, and parameter C lies between 0.35 and 0.45. The calculated values of critical nucleus at different undercoolings and interfacial energy for different materials are reported in Tables 2 and 3, respectively.

During the recent past, various attempts have been made to understand and explain the process of solidification of monotectic alloys [16, 17], particularly the influence of temperature. The role of wetting behavior in a phase separation process is of immense importance. In view of this, the applicability of Cahn wetting condition has been tested in the present case. The values of interfacial energy (Table 3) in the present case show applicability of wetting condition by satisfying the relation:

Table 2 Critical radius of DBB, PG, and their monotectic and eutectic

Undercooling ΔT/°C	Critical radius $\times 10^{-8}$/cm			
	DBB	PG	Monotectic	Eutectic
3.0	3.92		0.18	3.60
4.0	2.94		0.14	2.60
5.0	2.35	3.43	0.11	2.16
6.0	1.96	2.86	0.09	1.80
7.0	1.68	2.45		
8.0		2.15		
9.0		1.91		

Table 3 Interfacial energy of DBB, PG, and their eutectic and monotectic

Parameter	Interfacial energy $\times 10^{-6}$/kJ m^{-2}
σ_{SL_1} (PG)	50.53
σ_{SL_2} (DBB)	33.59
$\sigma_{\text{L}_1\text{L}_2}$ (Monotectic)	01.72
σ_{E} (Eutectic)	33.76

Table 4 Excess thermodynamic functions for the eutectic

Material	g^{E}/kJ mol^{-1}	h^{E}/kJ mol^{-1}	s^{E}/kJ mol^{-1} K^{-1}
Eutectic	−0.003	3.080	0.010

$$\sigma_{\text{SL}_2} < \sigma_{\text{SL}_1} + \sigma_{\text{L}_1\text{L}_2} \tag{4}$$

where σ is the interfacial energy between the interfaces denoted by the subscripts and the interfacial energy between two liquids,$\sigma_{\text{L}_1\text{L}_2}$ has been calculated using the equation

$$\sigma_{\text{L}_1\text{L}_2} = \sigma_{\text{SL}_1} + \sigma_{\text{SL}_2} - 2\sqrt{\sigma_{\text{SL}_1} \sigma_{\text{SL}_2}} \tag{5}$$

Excess thermodynamic functions

The deviation from the ideal behavior can best be expressed in terms of excess thermodynamic functions, namely,

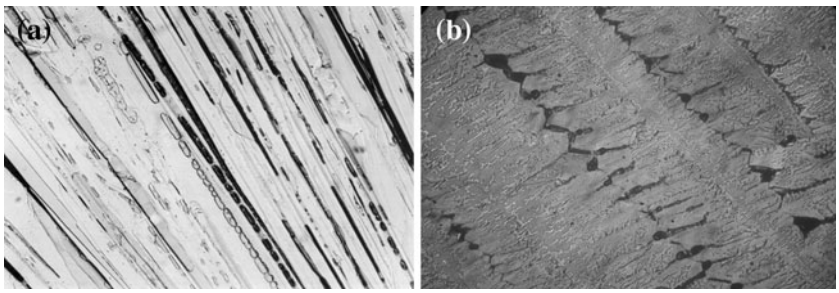

Fig. 3 Directionally solidify optical microphotograph of 1,4-dibromobenzene–pyrogallol monotectic (**a**) and eutectic (**b**)

excess free energy (g^{E}), excess enthalpy (h^{E}), and excess entropy (s^{E}) which give a more quantitative idea about the nature of molecular interactions. The excess thermodynamic functions [18] could be calculated using the following equations and the values are given in Table 4.

$$g^{E} = RT[x_1 \ln \gamma_1^1 + x_2 \ln \gamma_2^1] \tag{6}$$

$$h^{E} = -RT^2\left[x_1 \frac{\partial \ln \gamma_1^1}{\partial T} + x_2 \frac{\partial \ln \gamma_2^1}{\partial T}\right] \tag{7}$$

$$s^{E} = -R\left[x_1 \ln \gamma_1^1 + x_2 \ln \gamma_2^1 + x_1 T \frac{\partial \ln \gamma_1^1}{\partial T} + x_2 T \frac{\partial \ln \gamma_2^1}{\partial T}\right] \tag{8}$$

where γ_i^1, x_i and $\frac{\partial \ln \gamma_i^1}{\partial T}$ are activity coefficient in liquid state, the mole fraction, and variation of log of activity coefficient in liquid state as function of temperature of component i, respectively.

It is evident from Eqs. (6)–(8) that activity coefficient and its variation with temperature are required to calculate the excess functions. Activity coefficient (γ_i^1) could be evaluated using the equation

$$-\ln(x_i \gamma_i^1) = \frac{\Delta H_{fusi}}{R}\left(\frac{1}{T_E} - \frac{1}{T_i}\right) \tag{9}$$

where x_i, ΔH_{fusi}, T_i, and T_E are mole fraction, enthalpy of fusion, melting temperature of component i, and eutectic melting temperature, respectively. The variation of activity coefficient with temperature could be calculated by differentiating Eq. (9) with respect to temperature

$$\frac{\partial \ln \gamma_i^1}{\partial T} = \frac{\Delta H_{fusi}}{RT^2} - \frac{\partial x_i}{x_i \partial T} \tag{10}$$

$\partial x_i/\partial T$ in this expression can be evaluated by taking two points near the eutectic. The negative value of excess free energy, g^{E}, suggests that the interactions between unlike molecules are stronger than those between like molecules [15].

Microstructure

It is well known that in polyphase materials, the microstructure gives information about shape and size of the crystallites, which plays a very significant role in deciding about mechanical, electrical, magnetic, and optical properties of materials. The growth morphology of a eutectic system is controlled by the growth characteristics of the constituent phases. According to Hunt and Jackson [19], the type of growth from melts depends upon the interface roughness (α) defined by

$$a = \xi \Delta H_{fus}/RT \tag{11}$$

where ξ is a crystallographic factor which is generally equal to or less than one. The values of α are reported in Table 1. If $\alpha > 2$, the interface is quite smooth and the crystal develops with a faceted morphology. On the other hand, if $\alpha < 2$, the interface is rough and many sites are continuously available and the crystal develops with a non-faceted morphology. The value of α for parent component and binary in the present system, being more than 2 suggests the faceted morphologies of phases.

The unidirectional solidify microstructure of monotectic and eutectic are given in Fig. 3. The studied interfacial energy reveals the applicability of wetting condition for monotectic, i.e., both phases wet each other. Similar observation has been found as the microstructure of monotectic shows parallel array of lamellae and broken lamellae (Fig. 3a), while the eutectic of this system shows typical dendritic structure elongated in a particular direction (Fig. 3b). The closer view of the microstructure of eutectic also shows the secondary and tertiary growth fronts.

Conclusions

The experimentally determined phase diagram of 1,4-dibromobenzene–pyrogallol system shows the formation of a eutectic and a monotectic with 0.99 and 0.12 mol fractions of DBB, respectively. The consolute temperature was found to be 28.0 °C above the monotectic horizontal. The growth kinetics of pure components, the eutectic, and the monotectic determined at different undercoolings suggest that growth takes place according to the Hillig–Turnbull equation. The entropy of fusion, enthalpy of mixing, and interfacial energy for monotectic and eutectic were computed using the enthalpy of fusion values determined by the DSC method. The positive values of ΔH_{mix} for the eutectic suggests the quasi-eutectic structure in the binary eutectic melt, while the interfacial energies satisfy the relation,

$\sigma_{SL_2} < \sigma_{SL_1} + \sigma_{L_1L_2}$, which confirms the applicability of Cahn wetting condition to the present system. Microstructural investigation of monotectic shows the lamellae and broken lamellae, and the eutectic shows dendritic morphology.

Acknowledgements Authors sincerely thank the Board of Research in Nuclear Science, Department of Atomic Energy, Mumbai, India for financial support and the Head of the Department of Chemistry, B.H.U. Varanasi, for providing infrastructure facility.

References

1. Majumdar B, Chattopadhyay K. The Rayleigh instability and the origin of rows of droplets in the monotectic microstructure of zinc-bismuth alloys. Met Trans A. 1996;27(A):2053–7.
2. Chang TC, Hsu YT, Hon MH, Wang MC. Enhancement of the wettability and solder joint reliability at the Sn–9Zn–0.5Ag lead-free solder alloy–Cu interface by Ag precoating. J Alloys Compd. 2003;360:217–24.
3. Lin L, Rui T, Xueshan X. Development of bulk metallic glasses based on the Dy-Al binary eutectic composition. J Rare Earths. 2008;26(6):813–6.
4. Rice JW, Fu J, Suuberg EM. Anthracene + pyrene solid mixtures: eutectic and azeotropic character. J Chem Eng Data. 2010;55:3598–605.
5. Rai US, Rai RN. Physical chemistry of organic eutectics. J Therm Anal Calorim. 1998;53:883–93.
6. Gupta P, Agrawal T, Das SS, Singh NB. Solvent free reactions, reactions of nitrophenols in 8-hydroxyquinoline–benzoic acid eutectic melt. J Therm Anal Calorim. 2011;104:1167–76.
7. Dwivedi Y, Kant S, Rai SB, Rai RN. Synthesis, physicochemical and optical characterization of novel fluorescing complex: o-phenylenediamine-benzoin. J Fluoresc. 2011;21:1255–63.
8. Chen YP, Tang M, Kuo JC. Solid–liquid equilibria for binary mixtures of N-phenylacetamide with 4-aminoacetophenone, 3-hydroxyacetophe-none and 4-hydroxyacetophenone. Fluid Phase Equilib. 2005;232:182–8.
9. Ji HZ, Meng XC, Zhao HK. Solid + liquid) equilibrium of (4-chloro-2-benzofuran-1,3-dione + 5-chloro-2-benzofuran-1,3-dione. J Chem Eng Data. 2010;55:2590–3.
10. Sturz L, Witusiewicz VT, Hecht U, Rex S. Organic alloy systems suitable for the investigation of regular binary and ternary eutectic growth. J Cryst Growth. 2004;270:273–82.
11. Rai US, Pandey P. Some physicochemical studies on binary organic eutectic and monotectic alloys: p-dibromobenzene-m-aminophenol system. Mater Lett. 2004;58:2943–8.
12. Rai RN, Reddi RSB. Thermal, solid–liquid equilibrium, crystallization, and microstructural studies of organic monotectic alloy: 4,4′-Dibromobiphenyl–succinonitrile. Thermochim Acta. 2009; 496:13–7.
13. Hillig WB, Turnbull D. Theory of crystal growth in undercooled pure liquids. J Chem Phys. 1956;24:914.
14. Winegard WC. An introduction to solidification of metals. London: Institute of Metals Monograph; 1969 29: 67.
15. Rai US, Rai RN. Physical chemistry of organic eutectic and monotectic: hexamethylbenzene-succinonitrile system. Chem Mater. 1999;11:3031–6.
16. Ratke L, Diefenbach S. Liquid immiscible alloys. Mater Sci Eng. 1995;R15:263–347.
17. Singh NB, Rai US, Singh OP. Chemistry of eutectic and monotectic; phenanthrene-succinonitrile system. J Cryst Growth. 1985; 71:353–60.
18. Reddi RSB, Kumar SVSA, Rai US, Rai RN. Thermal, physicochemical and microstructural studies of binary organic eutectic systems. J Therm Anal Calorim. 2012;107:377–85.
19. Hunt JD, Jackson KA. Binary eutectic solidification. Trans Met Soc AIME. 1966;236:843–52.